frontiers | Frontiers in Energy Research

TYPE Original Research
PUBLISHED 13 September 2024
DOI 10.3389/fenrg.2024.1445092

OPEN ACCESS

EDITED BY
Yang Gao,
Shanghai Jiao Tong University, China

REVIEWED BY
Junjun Xu,
Nanjing University of Posts and Telecommunications, China
Lu Zhang,
China Agricultural University, China

*CORRESPONDENCE
Jiayi Han,
2201213350@stu.pku.edu.cn

RECEIVED 06 June 2024
ACCEPTED 29 July 2024
PUBLISHED 13 September 2024

CITATION
Ding R, Wang X, Qiu W, Yao Y, Xu H, Geng Y, Zhuo Z and Han J (2024) Modeling and scheduling of utility-scale energy storage toward high-share renewable coordination. *Front. Energy Res.* 12:1445092. doi: 10.3389/fenrg.2024.1445092

Modeling and scheduling of utility-scale energy storage toward high-share renewable coordination

Ran Ding[1,2], Xuanyuan Wang[1], Wei Qiu[1], Yiming Yao[1], Haixiang Xu[1], Yan Geng[1], Zhihuan Zhuo[3] and Jiayi Han[4]*

[1]State Grid Jibei Electric Power Co., Ltd., Beijing, China, [2]Department of Electrical Engineering, Tsinghua University, Beijing, China, [3]State Key Laboratory of Alternate Electrical Power System with Renewable Energy Sources, School of Electrical and Electronic Engineering, North China Electric Power University, Beijing, China, [4]Department of Industrial Engineering and Management, College of Engineering, Peking University, Beijing, China

As the integration of high-proportion renewable energy into the grid increases, the intermittency and uncertainty of renewable energy output significantly affect the safe and stable operation of the power system. Combining utility-scale energy storage technology with renewable coordination is one of the methods to address these issues. Compressed air energy storage (CAES) has garnered extensive attention due to its large capacity, long operational life, and clean, low-carbon advantages. Given the poor compressibility of air and its high critical point, using carbon dioxide as the working fluid in utility-scale energy storage systems can achieve higher energy storage density and cycle efficiency. Accordingly, this paper focuses on the study of utility-scale energy storage system modeling and scheduling methods considering carbon dioxide energy storage. It investigates Compressed Carbon Dioxide Energy Storage (CCES) systems, analyzes the operational framework of typical CCES systems, and sequentially establishes models for the energy storage process, energy release process, hot water tank operation, and gas storage tank operation. Based on this, it explores power system optimization dispatch methods considering CCES, incorporating the established models into an optimization dispatch model for power systems with high wind power penetration. Within the framework of a safe constraint unit commitment study, using the IEEE-30 nodes model, the effectiveness of the established models is validated. The case study results confirm the role of CCES in enhancing the absorption rate of renewable coordination. Moreover, under the same storage conditions, compared to, CCES offers greater charging and discharging power and higher energy storage density.

KEYWORDS

utility-scale energy storage, modeling, scheduling, renewable coordination, compressed carbon dioxide

1 Introduction

With the rapid depletion of global fossil energy resources, the issues of global warming and environmental pollution are becoming increasingly severe (Liu et al., 2020; Wang et al., 2020; Wang et al., 2023). Energy conservation, emission reduction, and the utilization of renewable energy have emerged as effective strategies to address the growing environmental

and energy challenges. To respond to global climate change and achieve the goals of peaking and neutralizing carbon dioxide emissions as soon as possible, it is necessary to further expand the coordination of renewable energy and actively realize a leapfrog development from fossil fuel-based power generation to clean and low-carbon energy sources (Dou et al., 2022; Ti et al., 2022; Zhang et al., 2022; Han et al., 2023; Yu et al., 2023). In 2020, China proposed the objectives of achieving carbon peak and carbon neutrality. The realization of these "dual carbon" goals necessitates proactive efforts in energy conservation and emission reduction, as well as vigorous development of renewable energy sources to reduce and offset our carbon emissions. Consequently, in recent years, China's renewable energy power generation has entered a phase of multiple growth.

Currently, the only large-capacity storage systems that can achieve 100 MW levels are pumped hydro storage systems and CAES systems (Zhang et al., 2023). However, the construction of pumped hydro storage plants requires special geographical conditions, and they have long construction periods, high initial investments, and can cause damage to the surrounding ecological environment during construction, severely restricting their development. In comparison, compressed air energy storage uses air as the compression medium in the system, not only is it safer, but the required geographical conditions are not as strict, and it has advantages in terms of construction period and investment cost. However, due to the lower compressibility of air compared to other gases (e.g., carbon dioxide), compressed air requires high thermodynamic parameters, necessitating more energy consumption in compressors during the compression process; and because of the low critical temperature of air (−140.5°C), liquid state energy storage places high demands on the equipment, making the technical and economic performance of compressed air energy storage systems often less than ideal (Jiang et al., 2022; Wang et al., 2022).

Compared to pumped hydro and CAES, compressed carbon dioxide energy storage systems, utilizing carbon dioxide as the compression medium, have several major advantages due to its excellent physical properties and environmental friendliness: (1) Compared to air, carbon dioxide has better compressibility, reducing energy consumption during the compression process; (2) The critical temperature and pressure of carbon dioxide are 30.98°C and 7.38 MPa, respectively, making it easier to liquefy than air and thus can be stored in tanks in liquid form, eliminating the need for specific geographical conditions; (3) The thermal cycle based on carbon dioxide is well-developed; (4) Using carbon dioxide as the working medium provides a new pathway for its large-scale application and offers a new effective indirect method for carbon dioxide emission reduction (Cavallo, 2001; Crotogino et al., 2001; Jiang et al., 2022; Wang et al., 2022). Based on these advantages, compressed carbon dioxide energy storage systems have shown better technical and economic performance, leading to an increasing number of proposals for such systems.

Morandin et al. (2012) proposed a hybrid system combining hot water and transcritical CO_2 circulation, which was optimized using pinch point analysis tools. Liu et al. (2016) presented a carbon energy storage system that utilized underground double reservoirs as carbon dioxide gas storage chambers, noting that transcritical systems exhibited higher cycle efficiency and energy density. A mathematical model of a compressed liquid CCES was established in (Wang et al., 2015). Parameter analysis was conducted and the results demonstrated that the incorporation of CCES significantly increased the penetration rate of renewable power. Xu et al. (2020) proposed a comparison with a liquid CAES revealed that the liquid CCES exhibited higher cycle efficiency. Furthermore, a trigeneration system based on the transcritical brayton cycle and energy storage system was proposed in (Liu et al., 2019). A thermodynamic model was developed to analyze its performance. Parameter analysis revealed that a lower thermal fluid utilization rate enhanced the cooling capacity, heating capacity, and total output energy of the system, making it more suitable for heating users than cooling users. Other studies have explored different aspects of CCES. For example, Bartela et al. (2021) presented the model of CCES utilizing a post-mining underground infrastructure, and CO_2 is stored under low pressure.

Existing studies often focus on the structural parameters and efficiency optimization of compressed carbon energy storage systems, with less research on the involvement of carbon storage systems in the optimization of power system scheduling. Therefore, this paper conducts research on the actual dispatch issues of utility-scale power systems involving carbon storage systems, based on the actual physical properties of carbon dioxide. The main contributions of this paper are as follows: 1) It proposes the system composition and operational framework of CCES utility-scale system, including compressors, expanders, CO_2 storage chambers, and thermal storage systems, and models the energy storage process, energy release process, thermal tank operation process, and gas storage tank operation process separately. 2) It employs a mixed-integer programming method to establish the corresponding mathematical model to study the optimal dispatch problem of power systems including compressed carbon dioxide energy storage.

2 Compressed carbon dioxide energy storage system modeling

This section presents the working principles and components of a CCES utility-scale system, including compressors, expanders, gas storage chambers, and thermal storage systems. Models are developed for the energy storage process, energy release process, thermal storage tank operation, and gas storage tank operation.

2.1 Principle of CCES

As shown in Figure 1, during low load periods in the power grid, compressors are used to compress low-pressure carbon dioxide stored in underground gas chambers to high-pressure state and deposit it within high-pressure gas reservoir. At the same time, a thermal storage medium recovers and stores the compression heat from the compressor units. During peak electricity usage periods in the power grid, the carbon dioxide stored in high-pressure gas chambers absorbs thermal energy and enters the expander units, utilizing the stored compression heat to drive multi-stage expanders for power generation. The carbon dioxide, after working through the expanders, enters the low-pressure gas chambers. The energy storage system's thermal storage/cooling units include cold

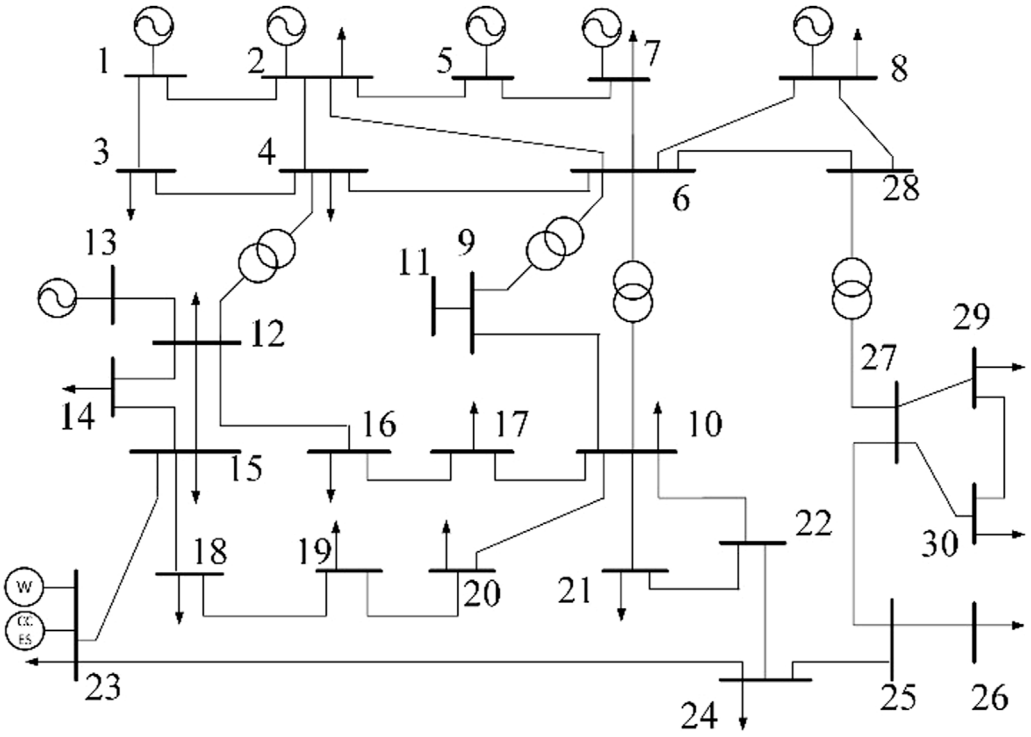

FIGURE 1
Topology of the IEEE 30-node System.

storage tanks, heat storage tanks, intercoolers between compressors, and reheaters between expander stages. When carbon dioxide is compressed, the thermal medium (water or another medium) in the cold tank is heated in the intercooler between compressors and then stored in the heat storage tank. When the expander is working, the high-temperature thermal medium from the heat storage tank enters the expander's reheater to heat the high-pressure carbon dioxide. The thermal medium, after releasing heat in the reheater, is recovered back to the cold storage tank.

2.2 Physical modeling of CCES

2.2.1 Charging and discharging power constraints

$$P_t^{\text{cces,cha}} = \dot{m}_t^c c_p \sum_{k=1}^{n_c} T_{k,t}^{\text{c,in}} \left(\beta_{k,t}^c \frac{r-1}{r} - 1 \right) \Big/ \eta_c$$

where $P_t^{\text{cces,cha}}$ represents the total charging power at time t; $\dot{m}_t^c$ represents the mass flow rate of carbon dioxide entering the compressor at time t; c_p is the constant pressure specific heat capacity of carbon dioxide; $T_{k,t}^{\text{c,in}}$ represents the inlet temperature of the k-th stage compressor. η_c denotes the isentropic efficiency of the compressor during the charging process. $\beta_{k,t}^{c\,\frac{r-1}{r}}$ represents the compression ratio for k-th compressor, satisfying the following equation:

$$\beta_{k,t}^c = \left(\frac{p_t^{\text{hp}}}{p_t^{\text{lp}}} \right)^{\frac{1}{n_c}}, k = 1, 2, \cdots, n_c$$

where p_t^{hp} and p_t^{lp} represent the pressure in the high and low-pressure gas storage chambers during time t respectively; n_c represents the total stages of compressors.

Discharge power is the sum of the power of each stage expander during the discharge process.

$$P_{k,t}^{\text{cces,dis}} = \dot{m}_t^e c_p \sum_{k=1}^{n_e} T_{k,t}^{\text{e,in}} \left(1 - \beta_{k,t}^e - \frac{\gamma - 1}{\gamma} \right) \eta_e$$

where $P_{k,t}^{\text{cces,dis}}$ represents the total discharging power at time t; $\dot{m}_t^e$ represents the mass flow rate of carbon dioxide entering the turbine at time t; $T_{k,t}^{\text{e,in}}$ represents the inlet temperature of the k-th turbine. η_e represents the isentropic efficiency of the turbine during the discharging process. $\beta_{k,t}^e$ signifies the compression ratio for the turbine at stage k, satisfying the following equation:

$$\beta_{k,t}^e = \left(\frac{p_t^{\text{hp}}}{p_t^{\text{lp}}} \right)^{\frac{1}{n_e}}, k = 1, 2, \cdots, n_e$$

where n_e represents the total stages of turbines.

The power consumption of the compressor and the work done by the expander are essentially determined by the inlet and outlet states of CO_2 and thermodynamic equations. Taking the compression process as an example, the ideal power consumption of the compressor is calculated by the difference in enthalpy values of CO_2 at the outlet and inlet, multiplied by the unit mass flow rate. This result is then divided by the isentropic efficiency and mechanical efficiency to obtain the actual power consumption. The difference in enthalpy values of CO_2 at the inlet and outlet is further expressed as

the product of the specific heat capacity at constant pressure and the temperature difference of CO_2.

2.2.2 Temperature constraints of CCES system

In this study, the CCES system employs multistage compression and expansion. It is evident that the temperature of the working medium is a crucial factor influencing the charging and discharging power of CCES system. Thus, accurately characterizing the temperature of carbon dioxide during the charging and discharging processes is an essential aspect of modeling CCES systems. The inlet and outlet temperatures of the compressors and expanders satisfy the following equations:

$$T_{k,t}^{\mathrm{c,out}} = T_{k,t}^{\mathrm{c,in}} \beta_{k,t}^{c} \frac{r-1}{r}$$

$$T_{k,t}^{\mathrm{e,out}} = T_{k,t}^{\mathrm{e,in}} \beta_{k,t}^{e} - \frac{r-1}{r}$$

$T_{k,t}^{\mathrm{c,out}}$ signifies the outlet temperatures for the k-th compressor during time t; $T_{k,t}^{\mathrm{e,out}}$ signifies the outlet temperatures for the k-th stage turbine during time t; γ is the specific heat ratio of carbon dioxide. its value is equivalent to the ratio of the specific heat at constant pressure over the specific heat at constant volume.

During the heat exchange process, the introduction of the heat exchanger effectiveness ε denotes the outlet temperature of the heat exchanger, and assuming equal specific heat capacities for the cold and hot fluids, the inlet temperatures of each stage compressor and expander can be expressed as:

$$\begin{cases} T_{1}^{\mathrm{c,in}} = T^{\mathrm{lp}} \\ T_{k,t}^{\mathrm{c,in}} = (1-\varepsilon) T_{k-1}^{\mathrm{c,in}} \beta_{k-1,t}^{c} \dfrac{r-1}{r} + \varepsilon T^{\mathrm{cold}} \quad k = 2, \cdots, n_c \end{cases}$$

$$\begin{cases} T_{1}^{\mathrm{e,in}} = T^{\mathrm{hp}} \\ T_{k,t}^{\mathrm{e,in}} = (1-\varepsilon) T_{k-1}^{\mathrm{e,in}} \beta_{k-1,t}^{e} - \dfrac{r-1}{r} + \varepsilon T^{\mathrm{hot}} \quad k = 2, \cdots, n_e \end{cases}$$

T^{lp} and T^{hp} respectively denote the temperatures of the low-pressure and high-pressure gas storage chambers; ε represents the effectiveness coefficient of the heat exchanger; T^{cold} and T^{hot} denote the temperatures of the cold and hot fluids respectively.

2.2.3 Constraints of gas storage chamber

According to existing literature, the gas storage chamber of CCES can utilize underground saline aquifers and abandoned mines. When employing these as storage chambers, it is essential to account for the upper and lower limits of the storage pressure. The gas volume and mass within the storage chamber are determined by the state from the previous cycle and the mass flow rate during the scheduling period. Given that the volume remains constant, the relationship between pressure constraints and gas mass is established using the CO_2 volume-pressure-temperature equation. Since the storage chamber exchanges heat with the external environment, it is considered an isothermal storage chamber. The CCES system comprises two gas storage chambers, high-pressure and low-pressure, each satisfying the following equations:

$$m_{t+1}^{\mathrm{hp}} = m_{t}^{\mathrm{hp}} - \dot{m}_{t}^{g} + \dot{m}_{t}^{c}$$

$$m_{t+1}^{\mathrm{lp}} = m_{t}^{\mathrm{lp}} + \dot{m}_{t}^{g} - \dot{m}_{t}^{c}$$

m_{t}^{hp} and m_{t}^{lp} individually denote the aggregate mass of the gas storage chambers at low and high pressure. Additionally, the gas storage chambers are subject to constraints on upper and lower pressure limits:

$$p_{min}^{\mathrm{lp}} \le p_{t}^{\mathrm{lp}} \le p_{max}^{\mathrm{lp}}$$

$$p_{min}^{\mathrm{hp}} \le p_{t}^{\mathrm{hp}} \le p_{max}^{\mathrm{hp}}$$

p_{min}^{lp} and p_{max}^{lp} respectively represent the lower and upper pressure limits of the low-pressure of CO_2 storage reservoir. p_{min}^{hp} and p_{max}^{hp} respectively denote the lower and upper limits of the high-pressure CO_2 storage reservoir.

2.2.4 Operating constraints of CCES system

$$v_{t}^{c} + v_{t}^{e} \le 1$$

v_{t}^{c} and v_{t}^{e} are binary variables representing whether the energy storage station is in a charging or discharging state.

2.3 Whole life cycle modeling of CCES

As a new type of power storage system, CCES has a long construction cycle and an operation income period of more than 10 years to decades, which makes the project balance period extended, and the economic benefits are not obvious in the short term. In order to comprehensively and accurately analyze and evaluate the technical and economic characteristics of the system, the economic status of the CCES system in the whole life cycle is studied.

Whole life cycle cost refers to the comprehensive expenses that may occur throughout the entire life cycle of equipment, from investment, operation, maintenance, to decommissioning. Whole life cycle analysis methods can effectively address the contradiction between equipment development and financial constraints, making it a strategic measure to enhance life cycle profitability. For system investment projects, life cycle cost modeling can, to some extent, predict the direct and indirect economic benefits of the project, providing a comprehensive analysis of the technical and economic aspects of system investment projects, thereby offering rational decision-making support for investors. According to the definition of life cycle cost, the production cost of an energy storage system consists of investment construction costs and operating costs.

$$C^{\mathrm{total}} = C^{\mathrm{Inv}} + C^{\mathrm{OM}}$$

The investment construction costs of a compressed carbon dioxide energy storage station primarily include the procurement costs of key equipment such as compressors, expanders, and gas storage chambers. The operating and maintenance costs include fixed maintenance costs, variable maintenance costs, electricity purchase costs, and personnel costs. Fixed maintenance costs are determined by the scale of the compressed carbon dioxide energy storage station, while variable maintenance costs are related to the energy throughput of the storage station. The electricity purchase cost of the energy storage system is derived from the off-peak

10.3389/fenrg.2024.1445092

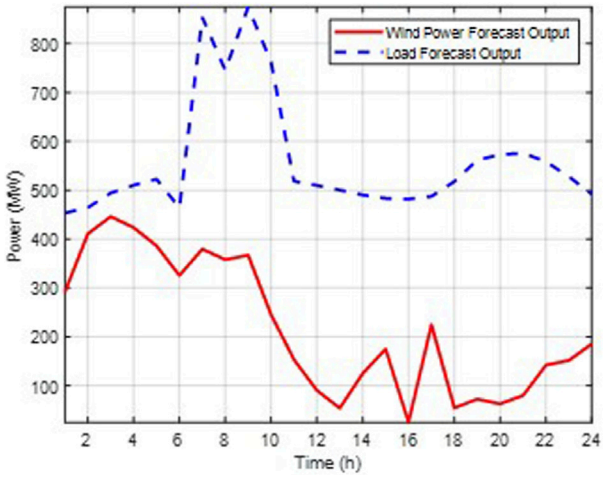

FIGURE 2
Forecast output of wind power and load.

electricity price and the total electricity consumption of the system over its life cycle.

$$\begin{cases} C^{\mathrm{OM}} = C^{\mathrm{fix}} + C^{var^{E\mathrm{Lab}}} \\ C^{\mathrm{fix}} = f^{\mathrm{OM,fix}} \cdot \left(P^{\mathrm{CCES,cha,\,max}} + P^{\mathrm{CCES,dis,\,max}}\right) \\ C^{\mathrm{var}} = f^{\mathrm{OM,var}} \cdot \sum_{y=1}^{N}\sum_{t=1}^{T} \frac{P_t^{\mathrm{CCES,cha}}}{(1+y)^d} \\ C^{E} = c^{\mathrm{pur}} \cdot \sum_{y=1}^{N}\sum_{t=1}^{T} P_t^{\mathrm{CCES,cha}} \end{cases}$$

3 Optimization scheduling model for power system including CCES system

An optimal scheduling model incorporating CCES and wind power is established. The optimization model minimizes the operational cost of the power system and considers operational constraints of CCES power stations, thermal power generation units, and wind power output.

3.1 Equations objective function of the optimization model

The objective function comprises the fuel costs for electricity generation and the startup costs of thermal power generation units. It is assumed that the operating cost of wind power generation is zero.

$$min\sum_{t=1}^{T}\left\{\sum_{t=1}^{N_G}\left[F_i\left(P_{i,t}^{G}\right) + S_{i,t}^{G}\right] + P_t^{\mathrm{cces}} C^{cces} + S_t{}^{cces} + \alpha P_t{}^{windlost}\right\}$$

T represents the total scheduling duration, N_G represents the number of thermal power generation units. F denotes the production cost function of thermal power generation units; $S_{i,t}^{G}$ denotes the cost associated with initiating and ceasing operations of thermal power generation units. C^{cces} represents the operational cost coefficient of the CCES unit, $S_t{}^{cces}$ is the startup and shutdown cost of the CCES power station; $P_t{}^{windlost}$ represents the curtailed wind power, and α denotes the wind curtailment penalty coefficient.

3.2 Constraints of the optimization model

3.2.1 Operational constraints of thermal power generation units

$$\begin{gathered} U_{i,t}^{G} P_{i,max}^{G} \le P_{i,t}^{G} \le U_{i,t}^{G} P_{i,max}^{G} \\ P_{i,t+1}^{G} - P_{i,t+1}^{G} \le v_i^{\mathrm{Gup}} \cdot \Delta t \\ P_{i,t}^{G} - P_{i,t+1}^{G} \le v_i^{\mathrm{Gdown}} \cdot \Delta t \\ T_{i,t}^{\mathrm{Gon}} \ge T_{i,min}^{\mathrm{Gon}} \\ T_{Gi,t}^{\mathrm{off}} \ge T_{i,min}^{\mathrm{Goff}} \end{gathered}$$

Equations delineate the upper and lower bounds of the unit's output, with $U_{i,t}^{G}$ signifying binary variables that reflect the unit's start-up and shut-down conditions. The unit's ramping limitations are outlined, where v_i^{Gup} and v_i^{Gdown} are the maximum and minimum ramping power thresholds of the unit, respectively. The minimum operational durations for starting up and shutting down the unit are defined by $T_{i,min}^{\mathrm{Gon}}$ and $T_{i,min}^{\mathrm{Goff}}$.

TABLE 1 Parameters of thermal power generation units.

Unit number	1	2	3	4	5	6
P_{max} (MW)	200	150	100	150	50	100
P_{min} (MW)	100	75	50	75	10	20
Fuel Cost Coefficient a ($/MW^2)	0.012	0.0014	0.0023	0.0032	0.0085	0.0046
Fuel Cost Coefficient b ($/MW)	8.66	9.66	12.1	13.4	19	12.69
Fuel Cost Coefficient c ($)	190	230	215	220	270	250
Ramp Rate (MW/min)	0.83	0.83	0.7	1.1	1.66	2.92
Minimum Start-Up/Shutdown Time (h)	8	8	4	4	1	1
Unit Start-Up/Shutdown Cost ($)	1,600	1,500	700	800	500	500

TABLE 2 Main parameters of CCES.

Parameters	Values	Unit
Rated power of total compressors	10	MW
Rated power of total turbines	10	MW
Machine efficiency of each compressor and turbine	0.98	—
Temperature of low presser chamber	305	K
Pressure range of low presser chamber	5–7	Mpa
Temperature of high presser chamber	350	K
Pressure range of high presser	16–24	Mpa
Volume of low presser chamber	15,000	m^3
Volume of low presser chamber	8,000	m^3
Isentropic efficiency of compressor	0.84	—
Isentropic efficiency of turbine	0.82	—
Rated ratio of compressors	2.7	—
Rated ratio of turbines	2.8	—

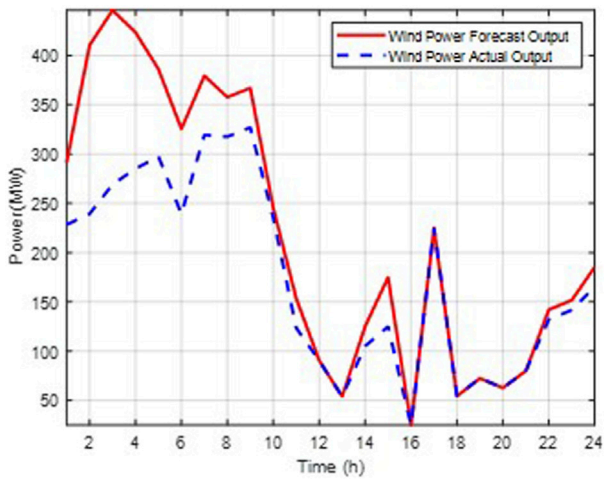

FIGURE 3
Output results of units without energy storage.

3.2.2 Operational constraints of thermal power generation units

$$0 \le P_t^{winds} \le P_t^{windf}$$

The actual dispatch output of wind power cannot exceed the forecasted wind power.

3.2.3 Constraint of system power balance

$$\sum_{i=1}^{N_G} P_{i,t}^{G} + P_t^{cces,dis} + P_{sW,t} = P_{Load,t} + P_t^{cces,cha}$$

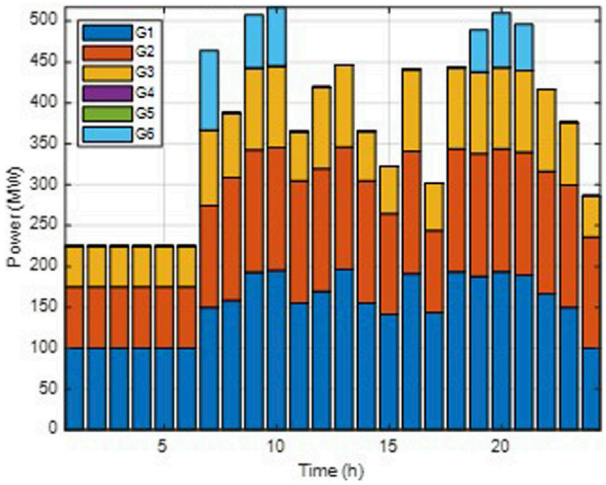

FIGURE 4
Output results of units without energy storage.

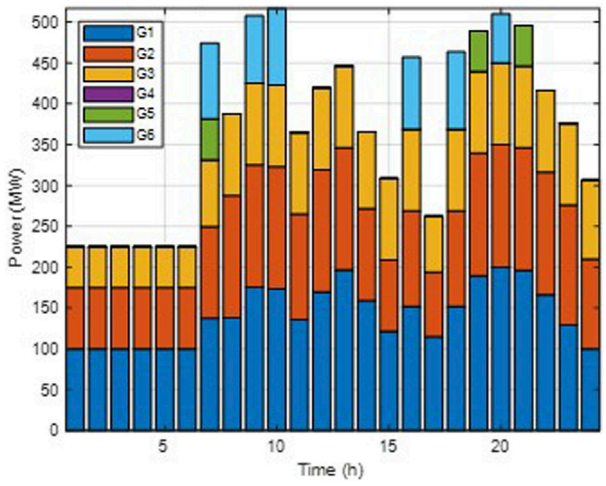

FIGURE 5
Output results of units with CAES system.

3.2.4 Constraint of system power flow

$$\boldsymbol{K}_p \boldsymbol{P}_{i,j,t}^{G} + \boldsymbol{K}_w \boldsymbol{P}_{j,t}^{wind} - \boldsymbol{K}_D \boldsymbol{D}_{j,t} = \boldsymbol{S}_F \boldsymbol{P}_L \ \forall i, \forall j, \forall t$$
$$0 <= \boldsymbol{P}_L <= \boldsymbol{P}_L^{max}$$

Equations calculate network power flows using the correlation matrix and transfer factor matrix, and constrain line power flows not to exceed limits.

4 Case studies

4.1 Description

This paper conducts case studies based on an improved IEEE 30-node system. The schematic diagram of the system structure is

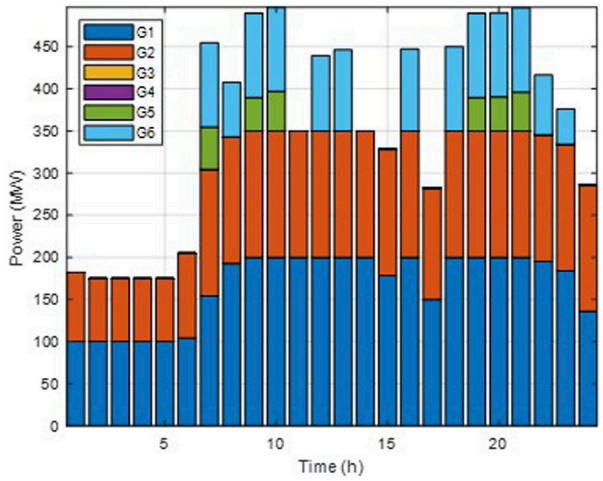

FIGURE 6
Output results of units with CCES system.

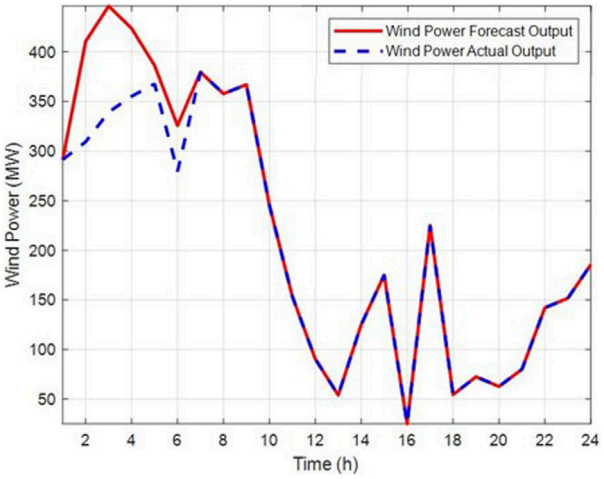

FIGURE 8
Wind power actual scheduling results with CCES.

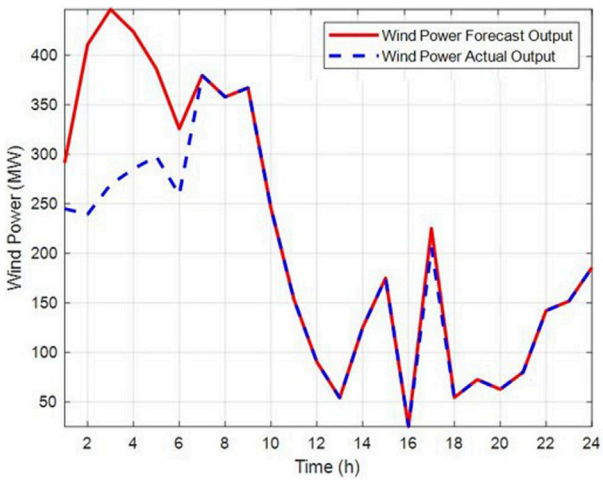

FIGURE 7
Wind power actual scheduling results with CAES.

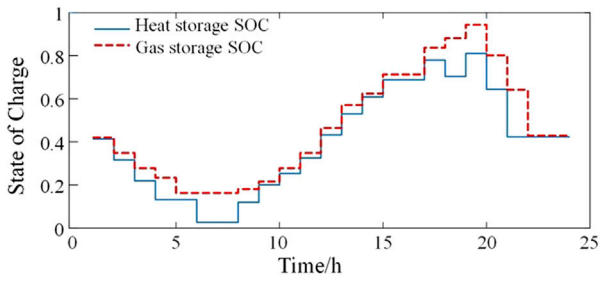

FIGURE 9
Typical daily energy storage status.

illustrated in Figure 2. A wind farm and a CCES power station are connected to node 23 of the original system. Economic comparative analysis is carried out considering three scenarios: no energy storage, carbon-containing energy storage power station, and compressed air energy storage power station, to analyze the total operating costs of the system. The Cplex toolbox in MATLAB 2020b is took for optimization scheduling modeling solving.

The IEEE 30-node system depicted in Figure 2 is studied over a 24-h period, comprising ten thermal power generation units labeled as G1 to G6, one wind power, and one CCES unit. The parameters of these units are presented in Tables 1, 2.

Figure 3 illustrates the hourly load forecast and wind power forecast over the 24-h period.

The analysis is conducted using the following three typical scenarios: Case 1: Without the inclusion of an energy storage power station; Case 2: With the inclusion of a CAES power station; Case 3: With the inclusion of a CCES power station.

4.2 Output results

Case 1. Without the inclusion of an energy storage power station.

As indicated by Figures 4, 5, during the hours with high actual wind power outputs, specifically the 5th, 7th, 9th, and 17th hours, with values of 297.672 MW, 320.11 MW, 327.01 MW, and 225.34 MW respectively, the system's scheduled wind power dispatch did not fully utilize the surplus wind power generation. This suggests that the system is willing to endure partial shutdowns of thermal power units along with the associated start-up and ramping costs to avoid substantial penalties for wind curtailment. However, due to the lack of energy storage facilities, a significant amount of wind power is still being wasted. This leads to an increased overall operational cost for the system.

Case 2. With the inclusion of a compressed air energy storage power station;

As depicted in Figures 6, 7, after the integration of a CAES system, the system experiences virtually no wind curtailment during the last 16 h, compared to Case 1, and significantly reduced wind curtailment in the first 8 h. The CAES system charges during periods of ample wind power supply and discharges during peak load periods, effectively performing peak shaving and valley filling.

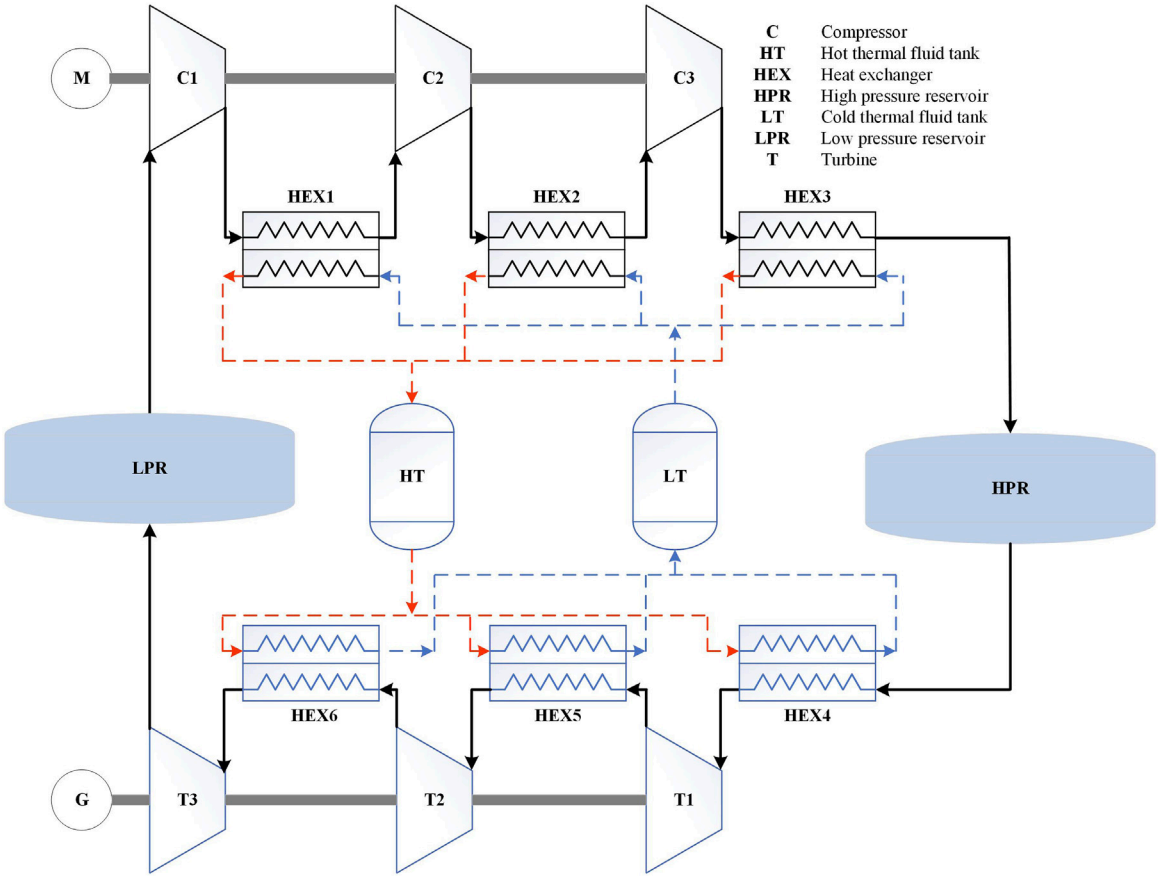

FIGURE 10
Schematic diagram of carbon energy storage system.

TABLE 3 Economic indicators.

Case number	Total operating costs ($)	Wind curtailment cost ($)
1	187,703	122,430
2	112,880	53,540
3	89,513	35,722

This mitigates the impact of wind power variability on the grid and subsequently reduces wind curtailment penalties.

Case 3. With the inclusion of a compressed carbon dioxide energy storage power station.

Figures 8, 9 illustrate that, following the implementation of a CCES system, the wind power absorption ratio during the initial 8 hours is significantly enhanced compared to Case 2. This improvement is attributed to carbon dioxide's ability to more easily surpass critical conditions and enter a supercritical state under the same operating conditions. With a higher fluid density, the working capacity of the medium is enhanced, leading to a substantial increase in both the charging/discharging power and storage capacity of the CCES. Consequently, this elevates the wind power absorption ratio.

Compared to traditional electrochemical energy storage, the state of charge (SOC) of a CCES system must consider both the pressure limits of the gas storage chamber and the maximum heat storage limits of the thermal storage system. To represent the SOC curve of a CCES, it is necessary to construct a dual-state curve of gas storage SOC and thermal storage SOC. The gas storage SOC is defined as the ratio of the mass of gas in the high-pressure storage chamber to the maximum storage mass, while the thermal storage SOC is defined as the ratio of the current heat storage amount to the maximum heat storage amount in the thermal storage system.

Figure 10 illustrates the changes in SOC within a single energy storage cycle under rated conditions for a compressed carbon dioxide energy storage system. Throughout the scheduling cycle, the maximum energy storage capacity of the system is constrained by both the pressure limits of the gas storage chamber and the heat limits of the thermal storage system. During the discharge process, the gas storage SOC decreases more rapidly, with the maximum discharge capacity limited by the pressure of the gas storage chamber. Conversely, during the

charging process, the thermal storage SOC increases more rapidly, with the maximum charging capacity constrained by the thermal storage limit. At the end of the scheduling cycle, the gas storage SOC returns to its initial state, allowing direct participation in the next cycle. The thermal storage system retains excess heat due to the heat absorption during the compression and charging process exceeding the heat release during the expansion and discharging process.

In summary, the reasonable configuration of a compressed carbon dioxide energy storage station needs to consider both the pressure limit of the gas storage chamber and the maximum heat storage limit of the thermal storage system. Additionally, the excess heat in the thermal storage system during the charge-discharge process validates that the compressed carbon dioxide energy storage system can provide thermal load supply under combined heat and power operation. This scheme can effectively reduce the operational costs of cogeneration units and improve the overall economic efficiency of the system.

4.3 Operating cost comparison

As shown in Table 3, in Case 1, due to the absence of storage units, the system is unable to absorb a significant amount of wind power during peak wind periods, leading to excessive wind curtailment penalties, particularly during initial 8 hours, when the curtailment reached 113 MW and 142 MW, respectively. Compared to Case 1, Case 2 sees reduced operating costs due to the participation of storage units in the dispatch. In Case 3, thanks to the high power and large capacity of the CCES station, wind curtailment is further reduced, and the system's operating costs continue to decrease.

5 Conclusion

This paper presents the system composition and operational framework of CCES system, including compressors, expanders, gas storage chambers, and thermal storage systems. It models the energy storage process, energy release process, thermal storage tank operation, and gas storage tank operation, respectively. A mixed integer programming approach is employed to establish the corresponding mathematical models, focusing on the optimal dispatch problem of power systems incorporating CCES. Case studies validate that under identical energy storage conditions, compared to CAES, the CCES system utilizing carbon dioxide as the working fluid possesses higher charging and discharging power and energy storage capacity. In power system optimization dispatch, it can maximize the absorption ratio of renewable energy, effectively reducing the operational costs of the system. As case study highlights the advantages of using CO_2 as a working fluid, there are also associated technical limitations. The large-scale geological sequestration of CO_2 is still under continuous development and improvement. The use of geological sequestration as a gas storage chamber is currently only studied theoretically and requires further validation in actual engineering applications. Additionally, due to the high-density characteristics of CO_2, existing compressors and expanders are mostly designed based on air. Therefore, the energy storage and discharge components suitable for CO_2 gas require further research.

Data availability statement

The original contributions presented in the study are included in the article/supplementary material, further inquiries can be directed to the corresponding author.

Author contributions

RD: Writing–original draft, Writing–review and editing. XW: Writing–original draft, Writing–review and editing. WQ: Writing–original draft, Writing–review and editing. YY: Writing–original draft, Writing–review and editing, Conceptualization, Investigation, Software, Data curation, Formal Analysis, Funding acquisition, Methodology, Project administration, Resources, Supervision, Validation, Visualization. HX: Writing–original draft, Writing–review and editing, Data curation, Methodology, Supervision, Conceptualization, Formal Analysis, Funding acquisition, Investigation, Project administration, Resources, Software, Validation, Visualization. YG: Writing–original draft, Writing–review and editing, Formal Analysis, Project administration, Validation, Conceptualization, Data curation, Funding acquisition, Investigation, Methodology, Resources, Software, Supervision, Visualization. ZZ: Writing–original draft, Writing–review and editing, Formal Analysis, Project administration, Validation, Conceptualization, Data curation, Funding acquisition, Investigation, Methodology, Resources, Software, Supervision, Visualization. JH: Writing–review and editing.

Funding

The author(s) declare that financial support was received for the research, authorship, and/or publication of this article. This work was supported by State Grid Corporation of China (No. 5100-202214502A-3-0-SF).

Conflict of interest

Authors RD, XW, WQ, YY, HX, and YG were employed by State Grid Jibei Electric Power Co., Ltd.

The remaining authors declare that the research was conducted in the absence of any commercial or financial relationships that could be construed as a potential conflict of interest.

The authors declare that this study received funding from State Grid Corporation of China. The funder had the following involvement in the study: Study design, data collection and the writing of this article.

Publisher's note

References

Bartela, Ł., Skorek-Osikowska, A., Dykas, S., and Stanek, B. (2021). Thermodynamic and economic assessment of compressed carbon dioxide energy storage systems using a post-mining underground infrastructure. *Energy Convers. Manag.* 241, 114297. doi:10.1016/j.enconman.2021.114297

Cavallo, A. J. E. (2001). Energy storage technologies for utility scale intermittent renewable energy systems. *J. Sol. Energy Eng.* 123 (4), 387–389. doi:10.1115/1.1409556

Crotogino, F., Mohmeyer, K.-U., and Scharf, R. J. O. (2001). "Huntorf CAES: more than 20 years of successful operation," in Solution mining research institute (SMRI) spring meeting. Orlando. FL.

Dou, X., Wang, Y., Ciais, P., Chevallier, F., Davis, S. J., Crippa, M., et al. (2022). Near-real-time global gridded daily CO2 emissions. *Innovation* 3 (1), 100182. doi:10.1016/j.xinn.2021.100182

Han, J., Wang, J., He, Z., An, Q., Song, Y., Mujeeb, A., et al. (2023). Hydrogen-powered smart grid resilience. *Energy Convers. Econ.* 4 (2), 89–104. doi:10.1049/enc2.12083

Jiang, K., Wang, P., Wang, J., and Liu, N. (2022). Reserve cost allocation mechanism in renewable portfolio standard-constrained spot market. *IEEE Trans. Sustain. Energy* 13 (1), 56–66. doi:10.1109/tste.2021.3103853

Liu, H., He, Q., Borgia, A., Pan, L., and Oldenburg, C. M. (2016). Thermodynamic analysis of a compressed carbon dioxide energy storage system using two saline aquifers at different depths as storage reservoirs. *Energy Convers. Manag.* 127, 149–159. doi:10.1016/j.enconman.2016.08.096

Liu, Z., Cao, F., Guo, J., Liu, J., Zhai, H., and Duan, Z. (2019). Performance analysis of a novel combined cooling, heating and power system based on carbon dioxide energy storage. *Energy Convers. Manag.* 188, 151–161. doi:10.1016/j.enconman.2019.03.031

Liu, Z., Yang, X., Jia, W., Li, H., and Yang, X. J. J. o. E. S. (2020). Justification of CO2 as the working fluid for a compressed gas energy storage system: a thermodynamic and economic study. *J. Energy Storage* 27, 101132. doi:10.1016/j.est.2019.101132

Morandin, M., Maréchal, F., Mercangöz, M., and Buchter, F. (2012). Conceptual design of a thermo-electrical energy storage system based on heat integration of thermodynamic cycles–Part B: alternative system configurations. *Energy* 45 (1), 386–396. doi:10.1016/j.energy.2012.03.033

Ti, B., Wang, J., Li, G., and Zhou, M. (2022). Operational risk-averse routing optimization for cyber-physical power systems. *CSEE J. Power Energy Syst.* 8 (3), 801–811. doi:10.17775/CSEEJPES.2021.00370

Wang, J., An, Q., Zhao, Y., Pan, G., Song, J., Hu, Q., et al. (2023). Role of electrolytic hydrogen in smart city decarbonization in China. *Appl. Energy* 336, 120699. doi:10.1016/j.apenergy.2023.120699

Wang, J., Wu, Z., Du, E., Zhou, M., Li, G., Zhang, Y., et al. (2020). Constructing a V2G-enabled regional energy Internet for cost-efficient carbon trading. *CSEE J. Power Energy Syst.* 6 (1), 31–40. doi:10.17775/CSEEJPES.2019.01330

Wang, M., Zhao, P., Wu, Y., and Dai, Y. (2015). Performance analysis of a novel energy storage system based on liquid carbon dioxide. *Appl. Therm. Eng.* 91, 812–823. doi:10.1016/j.applthermaleng.2015.08.081

Wang, S., Sun, P., Zhang, G., Gray, N., Dolfing, J., Esquivel-Elizondo, S., et al. (2022). Contribution of periphytic biofilm of paddy soils to carbon dioxide fixation and methane emissions. *Innovation* 3 (1), 100192. doi:10.1016/j.xinn.2021.100192

Xu, M., Zhao, P., Huo, Y., Han, J., Wang, J., and Dai, Y. (2020). Thermodynamic analysis of a novel liquid carbon dioxide energy storage system and comparison to a liquid air energy storage system. *J. Clean. Prod.* 242, 118437. doi:10.1016/j.jclepro.2019.118437

Yu, Y., Wang, J., Chen, Q., Urpelainen, J., Ding, Q., Liu, S., et al. (2023). Decarbonization efforts hindered by China's slow progress on electricity market reforms. *Nat. Sustain.* 6, 1006–1015. doi:10.1038/s41893-023-01111-x

Zhang, H., Liang, S., Wu, K., Qiu, Y., Cai, Y., Chan, G., et al. (2022). Using agrophotovoltaics to reduce carbon emissions and global rural poverty. *Innovation* 3 (6), 100311. doi:10.1016/j.xinn.2022.100311

Zhang, T., Wang, J., Wang, H., Ruiyang, J., Li, G., and Zhou, M. (2023). On the coordination of transmission-distribution grids: a dynamic feasible region method. *IEEE Trans. Power Syst.* 38 (2), 1857–1868. doi:10.1109/tpwrs.2022.3197556